

Electronic supplementary data to accompany

**Luminescent Cu(I) complexes with bisphosphane and halogen-substituted
2,2'-bipyridine ligands**

Sarah Keller,^a Alessandro Prescimone,^a Henk Bolink,^b Michele Sessolo,^b Giulia Longo,^b Laura Martínez-Sarti,^b José M. Junquera-Hernández,^b Edwin C. Constable,^a Enrique Ortí^{*b} and Catherine E. Housecroft^{*a}

^aDepartment of Chemistry, University of Basel, BPR 1096, Mattenstrasse 24a, CH-4058 Basel, Switzerland; email: catherine.housecroft@unibas.ch

^bInstituto de Ciencia Molecular, Universidad de Valencia, 46980 Paterna (Valencia), Spain; email: enrique.orti@uv.es

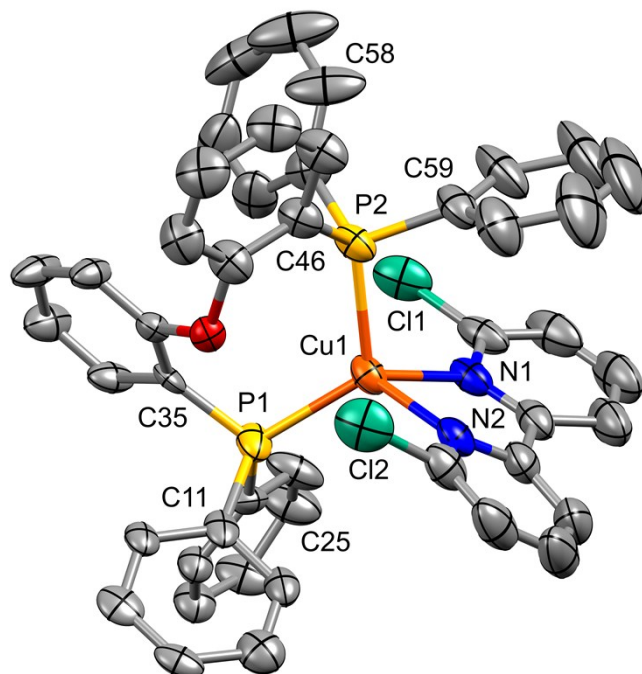


Fig. S1 Structure of the $[\text{Cu}(\text{POP})(6,6'\text{-Cl}_2\text{bpy})]^+$ cation in $[\text{Cu}(\text{POP})(6,6'\text{-Cl}_2\text{bpy})]\text{[PF}_6]$. The POP ligand is disordered over two sites (50:50 occupancies) and only one site is shown; four disordered aromatic rings were refined as rigid bodies. Ellipsoids plotted at 50% probability level, H atoms omitted.

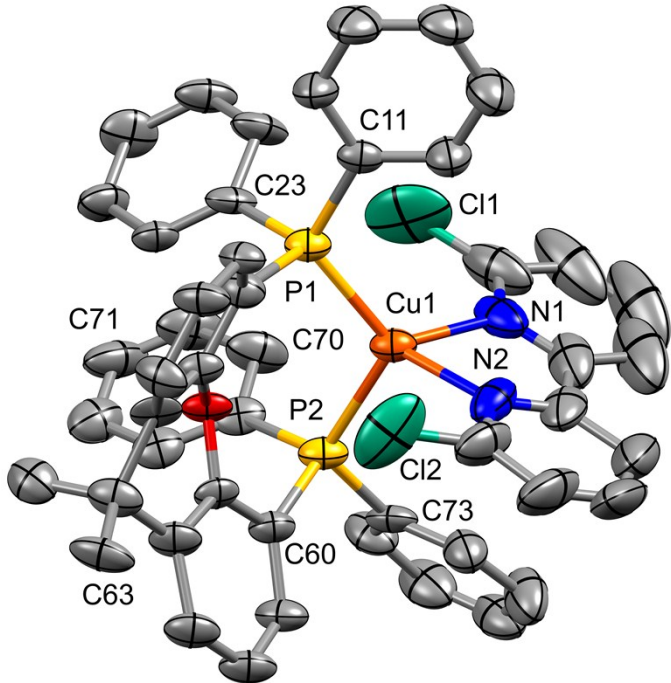


Fig. S2 Structure of the $[\text{Cu}(\text{xantphos})(6,6'\text{-Cl}_2\text{bpy})]^+$ cation in $[\text{Cu}(\text{xantphos})(6,6'\text{-Cl}_2\text{bpy})]\text{[PF}_6\text{]}\cdot\text{CH}_2\text{Cl}_2$. The xantphos ligand is disordered over two sites (50:50 occupancies). Ellipsoids plotted at 50% probability level, H atoms omitted.

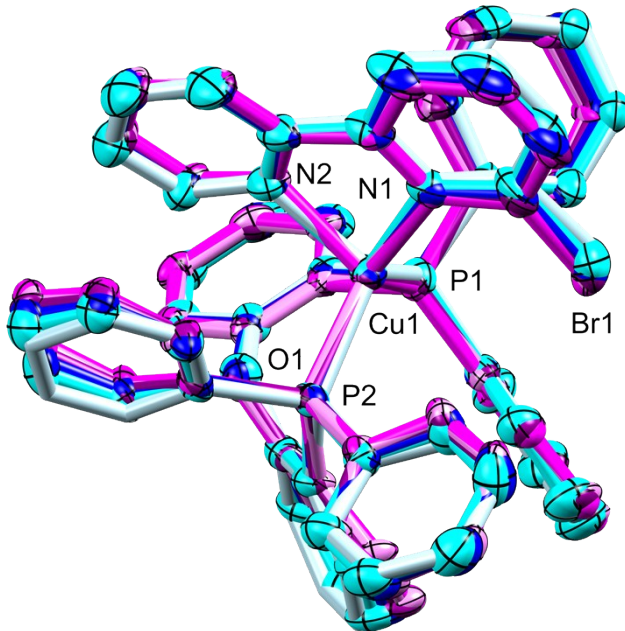


Fig. S3 Structure of the $[\text{Cu}(\text{POP})(6\text{-Brbpy})]^+$ cation in $[\text{Cu}(\text{POP})(6\text{-Brbpy})]\text{[PF}_6\text{]}$ under increasing pressure (0.16 to 4.5 GPa). Colour change from violet to light blue with increasing pressure. H atoms omitted, and ellipsoids are plotted at 50% probability level except for the highest pressure (4.5 GPa) structure which was refined anisotropically. The Cu–N and Cu–P bond distances decrease slightly as the pressure increases; e.g. Cu1–P1 changes from 2.250(6) Å at 0.16 GPa to 2.170(3) Å at 4.5 GPa, and Cu1–N2 from 2.110(14) to 2.017(4) Å, and the angle between the planes of the CuP_2 and CuN_2 units decreases from 83.63° to 86.09°.

Table S1 Experimental details for ambient and high pressure single crystal X-ray diffraction-measurements performed on [Cu(POP)(6-Brbpy)][PF₆].

For all the structures: C₄₆H₃₅BrCuF₆N₂OP₃, M_r = 982.16, monoclinic, P2₁/c, Z = 4.

	P ₀			
CCDC code	1535141	1584757	1584754	1584752
Crystal data				
Temperature (K)	123	293	293	293
Pressure (GPa)	ambient	0.16	1.30	1.80
a, b, c (Å)	15.3402 (6), 14.2344 (5), 19.2659 (7)	15.459 (10), 14.2430 (12), 19.413 (8)	15.123 (8), 13.6502 (10), 18.868 (7)	14.960 (8), 13.2757 (8), 18.724 (6)
β (°)	90.9159 (12)	90.03 (6)	91.32 (5)	92.23 (5)
V (Å ³)	4206.34 (15)	4274 (3)	3894 (2)	3716 (2)
D _x (Mg m ⁻³)	1.551	1.526	1.675	1.755
Radiation type	Cu Ka	Synchrotron, I = 0.48590 Å	Synchrotron, I = 0.48590 Å	Synchrotron, I = 0.48590 Å
m (mm ⁻¹)	3.49	1.62	1.78	1.87
Crystal size (mm)	0.12 × 0.10 × 0.08	0.04 × 0.02 × 0.02	0.04 × 0.02 × 0.02	0.04 × 0.02 × 0.02
Data collection				
Diffractometer	Bruker Kappa Apex2	Pilatus 300K	Pilatus 300K	Pilatus 300K
Radiation source	Cu Ka	Diamond Light Source Beamline I19	Diamond Light Source Beamline I19	Diamond Light Source Beamline I19
Monochromator	Graphite	Double crystal Silicon 111	Double crystal Silicon 111	Double crystal Silicon 111
Absorption correction	Multi-scan SADABS (Siemens, 1996)	Multi-scan CrysAlis PRO 1.171.38.41 (Rigaku Oxford Diffraction, 2015) Empirical absorption correction using spherical harmonics, implemented in	Multi-scan CrysAlis PRO 1.171.38.41 (Rigaku Oxford Diffraction, 2015) Empirical absorption correction using spherical harmonics, implemented in	Multi-scan CrysAlis PRO 1.171.38.41 (Rigaku Oxford Diffraction, 2015) Empirical absorption correction using spherical harmonics, implemented in

		SCALE3 ABSPACK scaling algorithm.	SCALE3 ABSPACK scaling algorithm.	SCALE3 ABSPACK scaling algorithm.
T_{\min}, T_{\max}	0.65, 0.76	0.033, 1.000	0.079, 1.000	0.074, 1.000
No. of measured, independent and observed [$ I > 2.0\sigma(I)$] reflections	35307, 7329, 7293	26697, 6179, 2242	24175, 5560, 2847	22897, 5151, 2851
R_{int}	0.022	0.157	0.119	0.115
$(\sin \theta / \lambda)_{\max} (\text{\AA}^{-1})$	0.595	0.799	0.797	0.797
Refinement				
$R[F^2 > 2\sigma(F^2)], wR(F^2), S$	0.028, 0.067, 0.89	0.095, 0.364, 1.08	0.071, 0.238, 1.01	0.067, 0.102, 1.13
No. of reflections	7329	6128	5534	5126
No. of parameters	541	541	445	445
No. of restraints	0	584	584	598
H-atom treatment	H-atom parameters constrained	H-atom parameters constrained	H-atom parameters not refined	H-atom parameters not refined
$\Delta\varphi_{\max}, \Delta\varphi_{\min} (\text{e \AA}^{-3})$	0.88, -0.39	1.19, -1.46	0.73, -0.72	0.74, -0.96

CCDC code	1584753	1584755	1584756
Crystal data			
Temperature (K)	293	293	293
Pressure (GPa)	3.50	4.20	4.50
$a, b, c (\text{\AA})$	14.765 (8), 12.9897 (9), 18.629 (6)	14.652 (7), 12.7677 (9), 18.624 (6)	14.622 (6), 12.6860 (8), 18.613 (6)
$\beta (\text{^\circ})$	92.14 (5)	91.96 (5)	92.10 (4)
$V (\text{\AA}^3)$	3570 (2)	3482 (2)	3450.3 (19)
$D_x (\text{Mg m}^{-3})$	1.827	1.873	1.891
Radiation type	Synchrotron, $\lambda = 0.48590 \text{\AA}$	Synchrotron, $\lambda = 0.48590 \text{\AA}$	Synchrotron, $\lambda = 0.48590 \text{\AA}$
$m (\text{mm}^{-1})$	1.94	1.99	2.01
Crystal size (mm)	$0.04 \times 0.02 \times 0.02$	$0.04 \times 0.02 \times 0.02$	$0.04 \times 0.02 \times 0.02$

Data collection			
Diffractometer	Pilatus 300K	Pilatus 300K	Pilatus 300K
Radiation source	Diamond Light Source Beamline I19	Diamond Light Source Beamline I19	Diamond Light Source Beamline I19
Monochromator	Double crystal Silicon 111	Double crystal Silicon 111	Double crystal Silicon 111
Absorption correction	Multi-scan <i>CrysAlis PRO</i> 1.171.38.41 (Rigaku Oxford Diffraction, 2015) Empirical absorption correction using spherical harmonics, implemented in SCALE3 ABSPACK scaling algorithm.	Multi-scan <i>CrysAlis PRO</i> 1.171.38.41 (Rigaku Oxford Diffraction, 2015) Empirical absorption correction using spherical harmonics, implemented in SCALE3 ABSPACK scaling algorithm.	Multi-scan <i>CrysAlis PRO</i> 1.171.38.41 (Rigaku Oxford Diffraction, 2015) Empirical absorption correction using spherical harmonics, implemented in SCALE3 ABSPACK scaling algorithm.
T_{\min} , T_{\max}	0.3168, 1.000	0.169, 1.000	0.225, 1.000
No. of measured, independent and observed [$ I > 2.0\sigma(I)$] reflections	22406, 4883, 2802	19321, 4281, 2817	20918, 4800, 3064
R_{int}	0.106	0.094	0.103
$(\sin \theta/\theta)_{\max}$ (\AA^{-1})	0.797	0.795	0.796
Refinement			
$R[F^2 > 2\sigma(F^2)]$, $wR(F^2)$, S	0.066, 0.092, 1.15	0.059, 0.088, 1.10	0.063, 0.097, 1.11
No. of reflections	4859	4276	4784
No. of parameters	445	445	415
No. of restraints	613	613	542
H-atom treatment	H-atom parameters not refined	H-atom parameters not refined	H-atom parameters not refined
$\Delta\varphi_{\max}$, $\Delta\varphi_{\min}$ ($e \text{\AA}^{-3}$)	0.88, -1.00	0.77, -0.72	0.97, -0.84

Computer programs: Apex2 (Bruker AXS, 2006), *CrysAlis PRO* 1.171.38.41k (Rigaku OD, 2015), *SUPERFLIP* (Palatinus & Chapuis, 2007), *CRYSTALS* (P. W. Betteridge, J. R. Carruthers, R. I. Cooper, K. Prout and D. J. Watkin, *J. Appl. Cryst.*, 2003, **36**, 1487), *CAMERON* (D. J. Watkin, C. K. Prout & L. J. Pearce. Oxford, UK, 1996).

Table S2 Selected structural parameters calculated at the B3LYP-D3/(def2svp + def2tzvp) level in CH₂Cl₂ solution for the [Cu(P⁺P)(N^NN)]⁺ complexes in their electronic ground state S₀ and in their first triplet excited state T₁.

Complex cation	Cu–P distance / Å (Cu1–P1; Cu1–P2)	Cu–N distance / Å (Cu1–N1; Cu1–N2)	P–Cu–P chelating angle / deg	N–Cu–N chelating angle / deg	Angle between P–Cu–P and N–Cu–N planes / deg	N–C–C–N torsion angle /deg
Ground State (S₀)						
[Cu(POP)(bpy)] ⁺	2.246; 2.284	2.096; 2.069	113.84	80.09	80.37	14.29
[Cu(xantphos)(bpy)] ⁺	2.269; 2.270	2.104; 2.068	114.40	79.75	86.94	3.23
[Cu(POP)(6,6'-Cl ₂ bpy)] ⁺	2.273; 2.291	2.160; 2.135	113.45	78.17	77.32	21.35
[Cu(xantphos)(6,6'-Cl ₂ bpy)] ⁺	2.271; 2.305	2.141; 2.145	119.27	77.38	86.72	6.76
[Cu(POP)(6-Brbpy)] ⁺	2.259; 2.288	2.110; 2.107	114.88	79.19	79.32	15.50
[Cu(xantphos)(6-Brbpy)] ⁺ ^a	2.280; 2.282	2.123; 2.096	113.74	78.71	87.38	3.30
[Cu(xantphos)(6-Brbpy)] ⁺ ^b	2.249; 2.299	2.112; 2.104	119.25	78.26	87.62	7.60
[Cu(POP)(6,6'-Br ₂ bpy)] ⁺	2.308; 2.281	2.153; 2.152	113.04	77.25	81.45	5.92
[Cu(xantphos)(6,6'-Br ₂ bpy)] ⁺	2.308; 2.282	2.160; 2.159	120.14	77.18	86.44	8.21
Triplet Excited State (T₁)						
[Cu(POP)(bpy)] ⁺	2.365; 2.334	1.982; 1.981	102.90	83.46	59.69	2.83
[Cu(xantphos)(bpy)] ⁺	2.350; 2.399	1.997; 1.981	105.92	83.06	57.53	1.99
[Cu(POP)(6,6'-Cl ₂ bpy)] ⁺	2.359; 2.330	2.068; 1.985	104.84	82.11	69.97	2.38
[Cu(xantphos)(6,6'-Cl ₂ bpy)] ⁺	2.360; 2.336	2.095; 1.989	105.69	81.40	77.17	5.42
[Cu(POP)(6-Brbpy)] ⁺	2.407; 2.341	2.000; 1.979	106.06	83.31	68.25	2.89
[Cu(xantphos)(6-Brbpy)] ⁺	2.384; 2.335	2.007; 1.973	106.76	82.58	67.93	3.24
[Cu(POP)(6,6'-Br ₂ bpy)] ⁺	2.381; 2.334	2.112; 1.982	104.69	81.50	73.21	5.38
[Cu(xantphos)(6,6'-Br ₂ bpy)] ⁺	2.370; 2.351	2.123; 1.994	105.43	81.18	78.88	7.20

^{a, b} Two different conformations were optimized for the [Cu(xantphos)(6-Brbpy)]⁺ complex that mainly differ in the orientation of the phenyl rings of the xantphos ligand (Fig. S3). The structure labeled with “a” is more similar to the reported X-Ray structure and is depicted in Fig. S3a, whereas the structure labeled with “b” corresponds to that displayed in Fig. S3b and appears at slightly lower energies. See the main text for details.

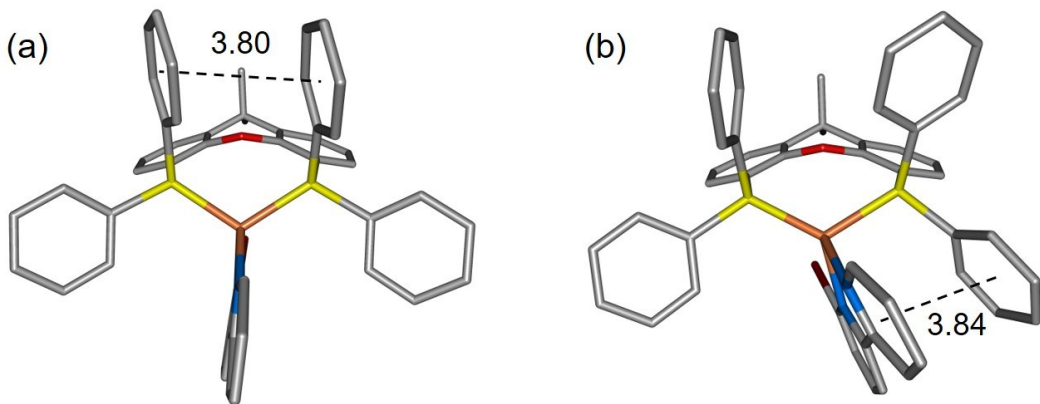


Fig. S4 Minimum-energy conformations calculated at the B3LYP-D3/(def2svp + def2tzvp) level in CH_2Cl_2 solution for $[\text{Cu}(\text{xantphos})(\text{6-Brbpy})]^+$. The conformation on the left (a) reproduces closely the X-ray structure reported for this complex. The conformation on the right (b) features a slightly lower energy. Hydrogen atoms are omitted for simplicity.

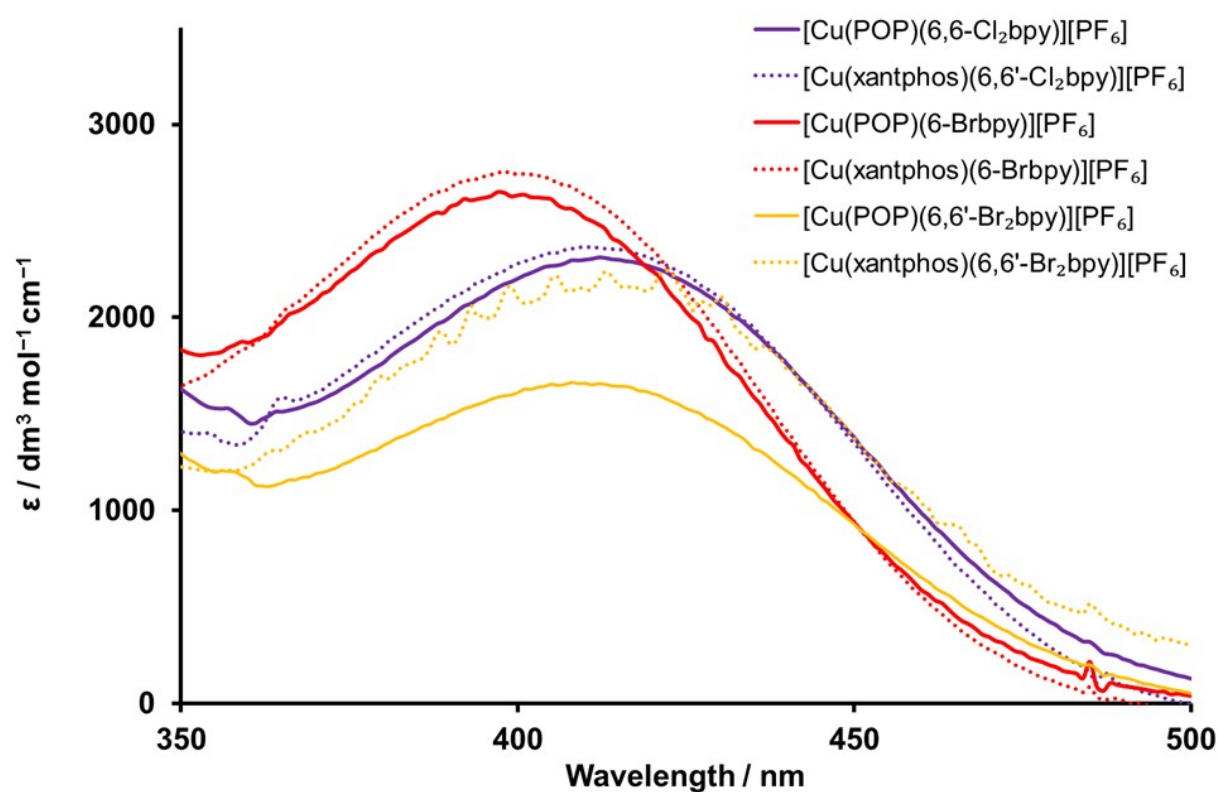


Fig. S5 Zoom into the low-energy MLCT region of the solution absorption spectra of the $[\text{Cu}(\text{P}^{\wedge}\text{P})(\text{bpy})][\text{PF}_6]$ complexes (CH_2Cl_2 , $2.5 \times 10^{-5} \text{ mol dm}^{-3}$).

Table S3 Vertical excitation energies (E) calculated at the TD-DFT B3LYP/(def2svp+def2tzvp) level for the lowest singlet (S_1) and triplet (T_1) excited states of complexes $[\text{Cu}(\text{P}^\wedge\text{P})(\text{N}^\wedge\text{N})]^+$ in CH_2Cl_2 solution. $S_0 \rightarrow S_1$ oscillator strengths (f) are given within parentheses. The energy of the T_1 state at its fully optimized TD-DFT geometry is given in the last column.

Complex cation	S_1	T_1	T_1 (relaxed)
	E (eV/nm) (f)	E (eV)	E (eV)
$[\text{Cu}(\text{POP})(\text{bpy})]^+$	2.800 / 443 (0.08)	2.544	1.220
$[\text{Cu}(\text{xantphos})(\text{bpy})]^+$	2.816 / 440 (0.10)	2.569	1.254
$[\text{Cu}(\text{POP})(6,6'\text{-Cl}_2\text{bpy})]^+$	2.618 / 474 (0.06)	2.407	1.423
$[\text{Cu}(\text{xantphos})(6,6'\text{-Cl}_2\text{bpy})]^+$	2.652 / 467 (0.07)	2.418	1.427
$[\text{Cu}(\text{POP})(6\text{-Brbpy})]^+$	2.724 / 455 (0.06)	2.486	1.410
$[\text{Cu}(\text{xantphos})(6\text{-Brbpy})]^+$	2.730 / 454 (0.07)	2.495	1.423
$[\text{Cu}(\text{POP})(6,6'\text{-Br}_2\text{bpy})]^+$	2.521 / 492 (0.04)	2.355	1.435
$[\text{Cu}(\text{xantphos})(6,6'\text{-Br}_2\text{bpy})]^+$	2.668 / 465 (0.06)	2.447	1.440

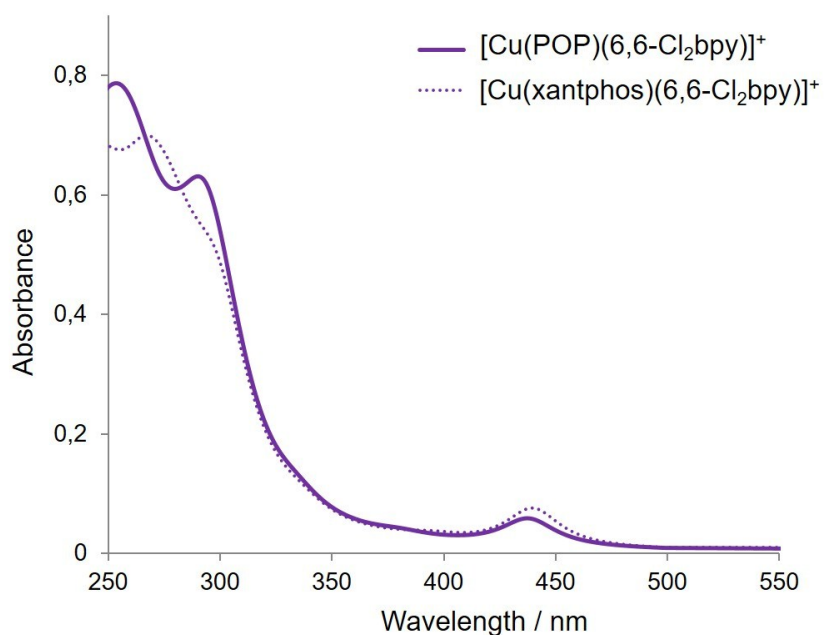


Fig. S6 TD-DFT simulations of the absorption spectra calculated at the B3LYP/(6-31G**+LANL2DZ) level of theory in CH_2Cl_2 for $[\text{Cu}(\text{POP})(6,6'\text{-Cl}_2\text{bpy})]^+$ and $[\text{Cu}(\text{xantphos})(6,6'\text{-Cl}_2\text{bpy})]^+$. The spectra were generated by convoluting each electronic transition with a Gaussian function of full-width-at-half-maximum FWHM = 30 nm.

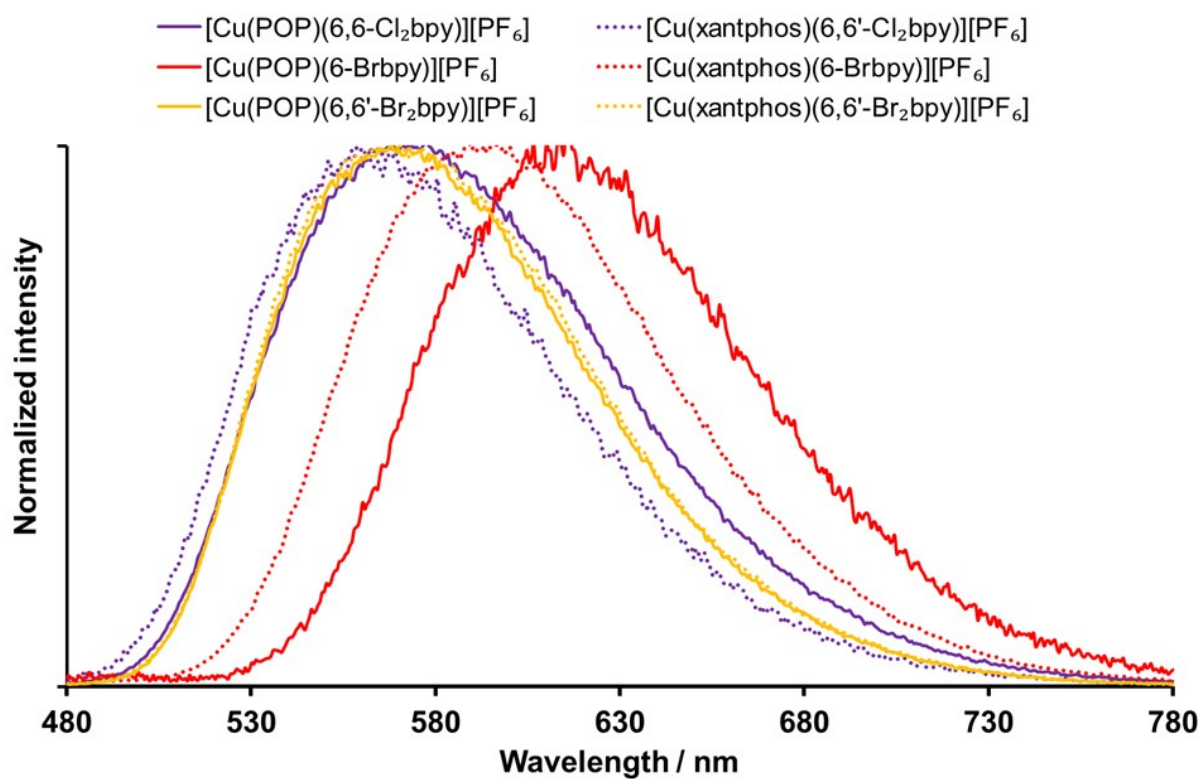


Fig. S7 Normalized emission spectra of the $[\text{Cu}(\text{P}^{\text{P}})(\text{bpy})]\text{[PF}_6]$ complexes in a frozen glass of Me-THF (77 K, $\lambda_{\text{exc}} = 410 \text{ nm}$).

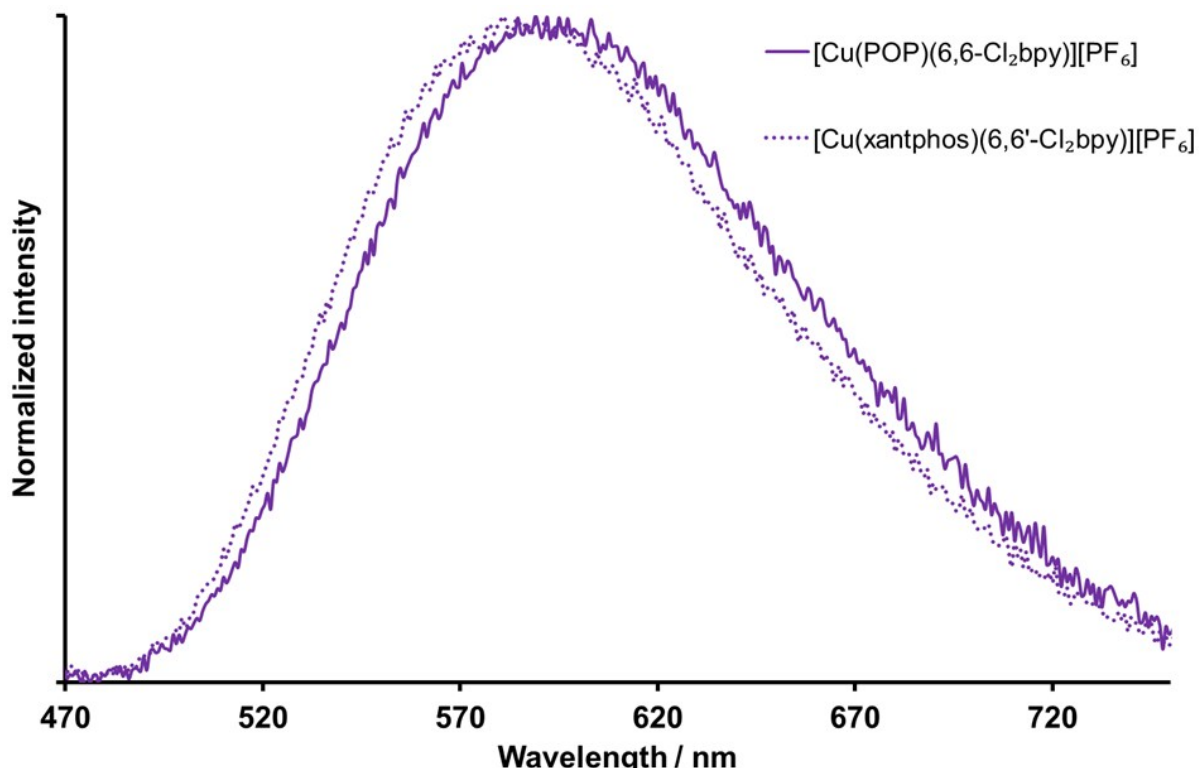


Fig. S8 Photoluminescence spectra of thin films composed of $[\text{Cu}(\text{P}^{\text{P}})(\text{6},\text{6}'\text{-Cl}_2\text{bpy})]\text{[PF}_6]$: $[\text{Emim}]\text{[PF}_6]$ at a 4:1 molar ratio ($\lambda_{\text{exc}} = 360 \text{ nm}$).

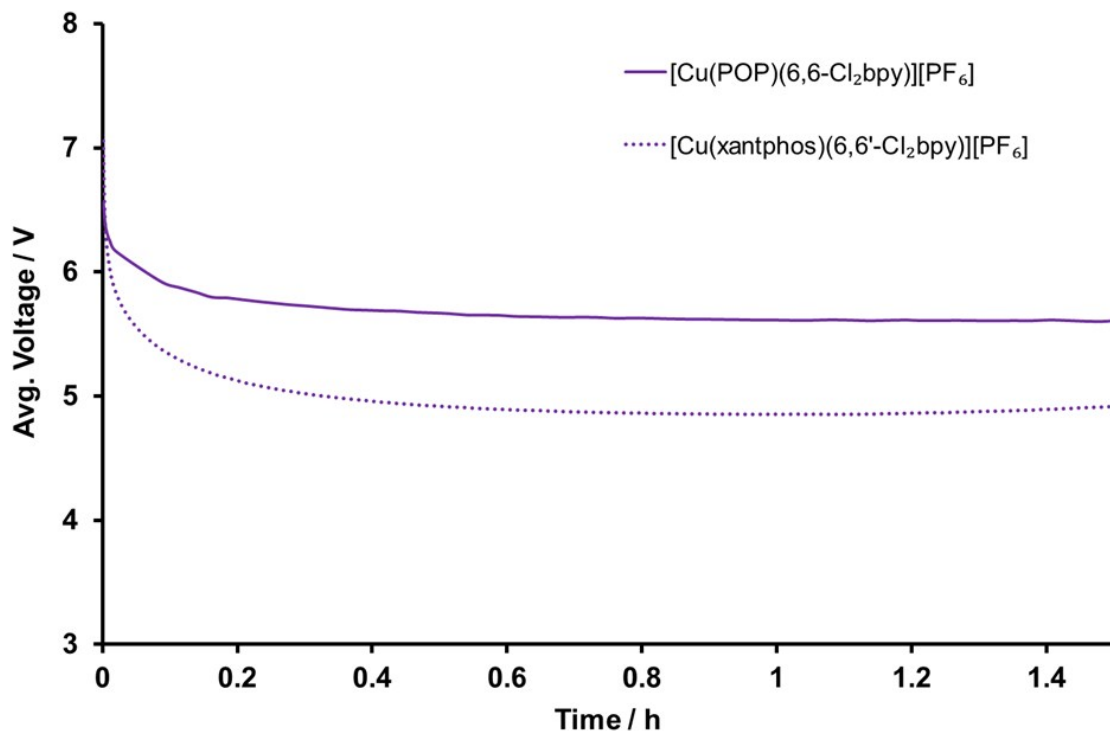


Fig. S9 Average voltage versus time characteristics measured for ITO/PEDOT:PSS/[Cu(P^AP)(N^NN)][PF₆]:[Emim][PF₆] 4:1/AI LECs operated at pulsed current (average density current 50 A m⁻², 1 kHz, 50% duty cycle, block wave).

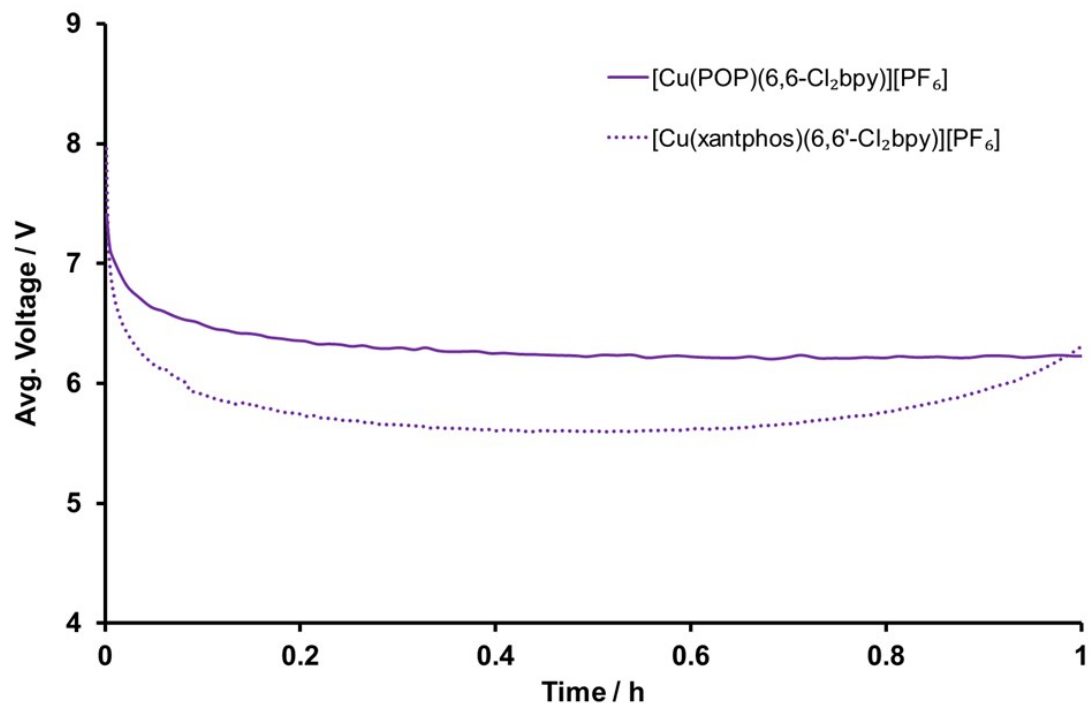


Fig. S10 Average Voltage versus time characteristics measured for ITO/PEDOT:PSS/[Cu(P^AP)^NN][PF₆]:[Emim][PF₆] 4:1/AI LECs operated at pulsed current (average density current 100 A m⁻², 1 kHz, 50% duty cycle, block wave).